

1 **A fungal endophyte induces local cell-wall mediated resistance in**
2 **wheat roots against take-all disease**

3 Tania Chancellor^{1,2}, Daniel P. Smith¹, Wanxin Chen¹, Suzanne J. Clark¹, Eudri Venter^{1,3},
4 Kirstie Halsey¹, Esther Carrera⁴, Vanessa McMillan^{1,5}, Gail Canning¹, Victoria Armer,¹ *Kim E.
5 Hammond-Kosack¹, Javier Palma-Guerrero^{1,6}

6 **Correspondence:** kim.hammond-kosack@rothamsted.ac.uk (KHK)

7 ¹Rothamsted Research, Strategic Areas: Protecting Crops and the Environment, Intelligent
8 Data Ecosystems, Plant Sciences for the Bioeconomy, West Common, Harpenden, AL5 2JQ,
9 UK.

10 **Current affiliations:**

11 ²Crop Science Centre, Department of Plant Sciences, University of Cambridge, 93 Lawrence
12 Weaver Road, Cambridge CB3 0LE, UK. ³JEOL (UK) Ltd. JEOL House, Silver Court,
13 Watchmead, Welwyn Garden City, Hertfordshire, AL7 1LT. ⁴Institute for Plant Molecular and
14 Cell Biology, University of Valencia, 46022 Valencia, Spain. ⁵NIAB, 93 Lawrence Weaver
15 Road, Cambridge CB3 0LE, UK. ⁶FIBL Research Institute of Organic Agriculture, Ackerstrasse
16 113, 5070 Frick, Switzerland.

17

18 **ORCID IDs:** 0000-0002-0867-7601 (JPG), 0000-0002-9699-485X (KHK), 0000-0002-3407-
19 1697 (TC), 0000-0001-5242-3812 (GC), 0000-0002-1008-520X (VA)

20

21 **Keywords:** wheat root transcriptomes, root endophyte, root pathogen, wheat defences, cell
22 wall modifications, fungal biocontrol

23

24

25

26

27

28

29

30

31

32 Abstract

33 Take-all disease, caused by the ascomycete fungus *Gaeumannomyces tritici*, is one of the
34 most important root diseases of wheat worldwide. The fungus invades the roots and destroys
35 the vascular tissue, hindering the uptake of water and nutrients. Closely related non-
36 pathogenic species in the *Magnaporthaceae* family, such as *Gaeumannomyces*
37 *hyphopodioides*, occur naturally in arable and grassland soils and have previously been
38 reported to reduce take-all disease in field studies. However, the mechanism of take-all
39 protection has remained unknown. Here, we characterise the root infection biologies of *G.*
40 *tritici* and *G. hyphopodioides* in wheat. We investigate the ultrastructure of previously
41 described “subepidermal vesicles” (SEVs), produced in wheat roots by non-pathogenic *G.*
42 *hyphopodioides*, but not by pathogenic *G. tritici*. We show that *G. hyphopodioides* SEVs share
43 key characteristics of fungal resting structures; containing a greater number of putative lipid
44 bodies and a significantly thickened cell wall compared to infection hyphae. We demonstrate
45 that take-all control is achieved via local but not systemic host changes in response to prior
46 *G. hyphopodioides* root colonisation. A time-course wheat RNA sequencing analysis revealed
47 extensive transcriptional reprogramming in *G. hyphopodioides* colonised tissues,
48 characterised by a striking downregulation of key cell-wall related genes, including cellulose
49 synthase (CESA), and xyloglucan endotransglucosylase/hydrolase (XTH) genes. In the
50 absence of take-all resistant wheat cultivars or non-virulent *G. tritici* strains, studying closely
51 related non-pathogenic *G. hyphopodioides* provides a much-needed avenue to elucidate take-
52 all resistance mechanisms in wheat.

53 Introduction

54 Wheat (*Triticum aestivum*) is one of the most important cereal crops worldwide, providing
55 around 20% of human caloric intake globally. Sustaining excellent root health is critical for the
56 acquisition of water and essential nutrients. As global temperatures continue to rise, root
57 health is predicted to face increasing threats from various soil-borne fungal pathogens
58 (Delgado-Baquerizo et al., 2020). The necrotrophic fungal pathogen *Gaeumannomyces tritici*,
59 belonging to the *Magnaporthaceae* family, is responsible for take-all disease, one of the most
60 important root problems of wheat crops worldwide (Freeman & Ward, 2004; Palma-Guerrero
61 et al., 2021). The disease drastically diminishes grain yields during heavy infection episodes.
62 However, due to the genetic intractability of *G. tritici*, both the pathogen and the cereal-
63 pathosystem remain understudied by the molecular plant-microbe interaction community.
64 Root-confined vascular infection by *G. tritici* results in the development of characteristic
65 necrotic lesions originating from the stele which severely disrupt root functions, causing
66 premature crop ripening and reduced grain yield/quality (Asher & Shipton, 1981; Huang et al.,
67 2001). Take-all fungal inoculum builds up in the soil following consecutive wheat crops, and
68 though recent surveys of take-all disease levels are lacking, yield losses of up to 60% have
69 been reported in the UK (McMillan et al., 2011). At present, take-all resistant wheat cultivars
70 are not commercially available, and current fungicide seed treatments do not provide complete
71 protection (Freeman et al., 2005).

72 Understanding root immunity is essential for the development of take-all resistant cultivars.
73 However, the classical model of immunity, characterised by the concerted effect of pathogen-
74 associated molecular pattern (PAMP) triggered immune responses (PTI) and effector
75 triggered immune responses (ETI), is predominantly based on foliar pathogens (Boller & Felix,
76 2009; Jones & Dangl, 2006; Pok et al., 2022). Roots must constantly interact with a diverse
77 soil microbiome and distinguish pathogenic microbes from, sometimes closely related, non-
78 pathogenic endophytes or beneficial symbionts (Thoms et al., 2021). How plants engage with
79 beneficial microorganisms while restricting damaging pathogens is regarded as one of the top
80 10 unanswered questions by the molecular plant-microbe-interaction (MPMI) research
81 community (Harris et al., 2020). The selective response of plants to microbes with different
82 lifestyles can be partly explained by the compartmentalisation of localised immune responses

83 in roots (Zhou et al., 2020), and the recognition of microbe-associated molecular patterns
84 (MAMPs), damage-associated molecular patterns (DAMPs) and pathogen-associated
85 molecular patterns (PAMPs) by multiple receptors (Thoms et al., 2021). However, further
86 comparative studies into endophytic and pathogenic plant infecting microbes are sorely
87 needed.

88 Several members of the *Magnaporthaceae* family are classified within the *Gaeumannomyces-*
89 *Phialophora* complex (Hernández-Restrepo et al., 2016). *Phialophora* species, such as
90 *Gaeumannomyces hyphopodioides*, occur naturally in grasslands and arable field sites,
91 though do not cause disease symptoms in arable crops (Deacon, 1973; Ulrich et al., 2000;
92 Ward & Bateman, 1999). For this reason, such species have been described as “non-
93 pathogenic”. Wheat colonisation by non-pathogenic *Magnaporthaceae* species can be easily
94 distinguished from wheat infection by pathogenic *G. tritici* due to the production of dark swollen
95 fungal cells in the root cortex. The swollen cells measure between 12 µm and 30 µm in
96 diameter, depending on the fungal species (Deacon, 1976a). These enigmatic structures have
97 been previously described as pigmented cells (Holden, 1976), growth cessation structures
98 (Deacon, 1976a) or subepidermal vesicles (SEVs) (Osborne et al., 2018). The closely related
99 rice leaf blast pathogen *Magnaporthe oryzae*, is also reported to form SEV-like structures in
100 cereal roots. *M. oryzae* can infect rice root tissues (Dufresne & Osbourn, 2001; Marcel et al.,
101 2010), producing brown spherical structures resembling SEVs in epidermal and cortical cells.
102 SEVs may form following growth cessation of a hyphal apex (Deacon, 1976a).

103 Prior colonisation by certain non-pathogenic *Magnaporthaceae* species is reported to provide
104 protection against take-all disease in field studies (Wong et al., 1996). Furthermore, Osborne
105 et al., (2018) demonstrated that certain elite winter wheat varieties have an improved ability to
106 promote *G. hyphopodioides* populations in field soils, suggesting that careful cultivar choice
107 during wheat rotations could provide a natural level of biocontrol. However, as far as we are
108 aware, disease protection by non-pathogenic *Magnaporthaceae* species has not been
109 reported in any recent publications, and the mechanism(s) underlying disease control remain
110 unknown. The existence of endophytic species conferring resistance against closely related
111 pathogens is not limited to the *Magnaporthaceae* family. Non-pathogenic strains in the
112 *Fusarium oxysporum* species complex are known to provide protection against Fusarium wilt
113 disease, a major disease caused by pathogenic *F. oxysporum* strains (de Lamo & Takken,
114 2020). This phenomenon, termed endophyte-mediated resistance (EMR), is reportedly
115 independent of jasmonic acid (JA), ethylene (ET) and salicylic acid (SA) signalling (Constantin
116 et al., 2019).

117 Here, we provide the first comparative analysis of wheat transcriptional responses to *G. tritici*
118 and *G. hyphopodioides* across key stages of early fungal infection. We characterise the
119 different fungal structures produced and some of the wheat cell wall changes occurring during
120 root infection. Our findings shed light on the distinct plant responses to these two closely
121 related root infecting fungi with contrasting lifestyles, and help to pinpoint localised
122 mechanisms for the control of take-all disease by *G. hyphopodioides*. Together, our findings
123 contribute to an improved understanding of wheat root resistance against take-all disease.

124 **Results**

125

126 **Hyphal interactions between *G. hyphopodioides* and *G. tritici***

127 To investigate the role of direct hyphal interaction in take-all control, a series of fungal
128 confrontation assays were conducted on potato dextrose agar (PDA) plates. Prior to hyphal
129 contact, the individual growth rates of *G. tritici* and *G. hyphopodioides* colonies did not
130 significantly differ from the dual colony controls (table S1). The same was true when the two
131 species were grown in a “sandwich” plate set-up (figure 1A, table S2), suggesting that prior to
132 hyphal contact, neither species produce diffusible antifungal compounds or volatile organic

133 compounds *in vitro*. When hyphae of the two fungal species interacted in confrontation assays,
134 a dark barrage was observed in the interaction zone (figure 1A). The observed barrage formed
135 1-2 days following hyphal interaction, perhaps suggesting that direct interaction causes hyphal
136 stress in at least one of the interacting species. A dark barrage was not observed when isolates
137 of the same species were confronted (figure S1).

138

139 **Pre-treatment with *G. hyphopodioides* provides local control against take-all disease**

140 To investigate the hypothesis that non-pathogenic *G. hyphopodioides* provides protection
141 against take-all disease by inducing wheat resistance, seedling co-inoculation experiments
142 were carried out under controlled environment conditions. *G. hyphopodioides* inoculum was
143 added to wheat seedlings (cv. Hereward) growing in pots 1 week prior, 2 weeks prior, at the
144 same time as, and 1 week after inoculation with pathogenic *G. tritici*. Characteristic black
145 necrotic root lesions were observed in *G. tritici* infected control plants. SEVs were observed
146 in plants co-inoculated with *G. hyphopodioides* (figure 1B). The data revealed a significant
147 reduction in both take-all disease levels and *G. tritici* fungal biomass in plants pre-treated with
148 *G. hyphopodioides* 2-weeks prior or 1-week prior to *G. tritici* inoculation (figure 1C, D). Hence,
149 even very early colonisation by *G. hyphopodioides* is sufficient for take-all control. These
150 findings were consistent with additional experiments involving a different *G. tritici* isolate (Gt
151 17LH(4)19d1) and wheat cultivar (cv. Chinese Spring) (figure S2).

152 Seedlings co-inoculated with *G. hyphopodioides* and *G. tritici* at the same time had no effect
153 on take-all disease levels or *G. tritici* fungal biomass. Importantly, adding *G. hyphopodioides*
154 after *G. tritici* resulted in increased levels of take-all disease and *G. tritici* fungal biomass
155 (figure 1C, D). Furthermore, the shoot and root dry biomass of plants in this latter treatment
156 were significantly reduced, indicating that seedling health is negatively affected when *G.*
157 *hyphopodioides* infections occur in addition to *G. tritici* infection (figure 1E, F). These findings
158 should be taken into careful consideration when evaluating the potential of *G. hyphopodioides*
159 as a biocontrol agent.

160 Split-root experiments were carried out to determine whether *G. hyphopodioides* provides
161 local or systemic protection against take-all disease. Significant disease reduction was
162 achieved only in roots which had been directly inoculated with *G. hyphopodioides* (LOC), and
163 not in systemic roots (SYS) which had not been directly inoculated with *G. hyphopodioides*
164 (figure 1G). Taken together, we demonstrate that local induced wheat resistance plays a
165 crucial role in the control of take-all disease by *G. hyphopodioides*, and this response is
166 consistent across both winter and spring wheat types.

167

168 **The differing infection biologies of *G. hyphopodioides* and *G. tritici* in wheat roots**

169 To study fungal infection processes during early root colonisation, wheat seedlings (cv.
170 Chinese Spring) were root inoculated with either *G. hyphopodioides* (NZ.129.2C.17) or *G.*
171 *tritici* (Gt 17LH(4)19d1) in an agar plate system. Plants were harvested at 2, 4 and 5 dpi to
172 capture key stages of fungal infection for later RNA-seq analysis. At 2 dpi, very few hyaline
173 runner hyphae were detected on the root surface of plants inoculated with either *G. tritici* or
174 *G. hyphopodioides*, and hyphae had not yet penetrated the epidermal cells in either interaction
175 (figure 2A, B). By 4 dpi, hyaline runner hyphae covered a greater area of the root surface
176 (figure S3) and hyphae were detected in epidermal and cortical cells of both *G. tritici* and *G.*
177 *hyphopodioides* inoculated roots (figure 2A, B). At 5 dpi, hyaline runner hyphae were detected
178 across a large area of the root surface (figure S3) in both fungal treatments. *G. tritici* hyphae
179 infected the stele, whereas *G. hyphopodioides* hyphal growth was arrested in the cortex (figure
180 2B). *G. hyphopodioides* hyphae were detected in cortical cells, from which SEVs were formed
181 (figure 2A). Newly formed SEVs could be visualised by wheat germ agglutinin (WGA) staining,
182 whereas mature SEVs, which were darker in colour, could not be visualised by WGA staining

183 (figure S4). *G. tritici* did not produce SEVs in wheat roots at any time point, and *G.*
184 *hyphopodioides* hyphae were not observed in the stele at any time point (figure S5).

185 To investigate the structure of mature SEVs, wheat plants (cv. Hereward) were inoculated with
186 *G. hyphopodioides* (NZ.129.2.17) in a seedling pot infection assay. Colonised plants were
187 harvested at 5 weeks post inoculation and imaged by transmission electron microscopy
188 (TEM). Comparative analysis of intraradical fungal hyphae and SEVs revealed that SEVs
189 contain a greater number of putative lipid bodies and a significantly thickened cell wall,
190 comprising two to three layers of differing densities (figure 3A, B). Multiple SEVs were often
191 observed in a single plant cell (figure 3C) and SEVs were often found appressed to the plant
192 cell wall (figure 3 D, E).

193

194 **Wheat transcriptional remodelling during fungal infection**

195 Three time-points (2, 4 and 5 dpi) were selected for RNA-seq analysis based on the stage of
196 fungal infection (figure S5). Principal Component Analysis (PCA) of sample distances
197 demonstrated a good level of clustering between biological replicates, though *G. tritici* infected
198 samples exhibited comparatively higher levels of variation (figure 4A). Gene expression levels
199 were compared between *G. tritici* infected or *G. hyphopodioides* colonised plants and the
200 uninoculated control plants at each time point individually. Full lists of the differentially
201 expressed genes (DEGs) can be found in table S3. As expected, the number of wheat DEGs
202 between the uninoculated control and *G. tritici* infected or *G. hyphopodioides* colonised plants
203 was low at 2 dpi (77 and 62, respectively). By 4 dpi, *G. tritici* infection and *G. hyphopodioides*
204 colonisation resulted in the differential expression of 1061 and 1635 wheat genes,
205 respectively. At 5 dpi, a striking number of wheat genes were DE in response to *G.*
206 *hyphopodioides* colonisation (7532), whereas the number of DEGs in response to *G. tritici*
207 infection (1074) showed little change compared to 4 dpi (figure 4B).

208 To investigate wheat transcriptional changes during the infection progression of *G.*
209 *hyphopodioides* compared to *G. tritici*, gene ontology (GO) enrichment analyses were carried
210 out on the sets of DEGs described above. At 2 dpi, genes involved in the terpenoid biosynthetic
211 process/metabolic process were upregulated in *G. tritici* inoculated roots. Meanwhile, genes
212 involved in the nicotianamine biosynthetic process/metabolic process were downregulated in
213 *G. hyphopodioides* inoculated roots (figure S6A, B). At 4 dpi, genes involved in the cinnamic
214 acid biosynthetic/metabolic process and the L-phenylalanine metabolic/catabolic process were
215 upregulated in *G. hyphopodioides* colonised wheat roots, suggesting that lignin biosynthesis
216 is important at this time point. However, these GO terms were not significantly enriched until
217 5 dpi in *G. tritici* infected roots, suggesting that lignin biosynthesis is also involved in the
218 defence response to *G. tritici*, though at a later stage than *G. hyphopodioides*. Other enriched
219 terms in *G. hyphopodioides* colonised plants at 5 dpi included response to wounding,
220 regulation of defence responses and regulation of the jasmonic acid (JA) signalling pathway.
221 Downregulated terms included gene expression, plant-type cell wall organisation or
222 biogenesis and RNA metabolic process (figure S6A, B).

223 Next, we compared the unique and shared wheat transcriptional responses to the two fungal
224 species. At 5 dpi, 97% of the genes which were DE in response to *G. tritici* infection were also
225 DE in response to *G. hyphopodioides* colonisation (figure 4C). Within this core set of genes at
226 5 dpi, highly enriched GO biological process terms included isoprenoid biosynthesis, plant
227 response to biotic stimulus and isoprenoid biosynthetic/metabolic process (figure 4D). The
228 plant response to biotic stimulus term comprised 42 DE genes, 14 of which encoded proteins
229 containing small cysteine-rich protein (SCP)-domains, often associated with pathogenesis-
230 related proteins. Six genes encoded chitinases, two encoded wound induced proteins (WIN)
231 and a further four encoded protein kinase domain-containing proteins, thus indicating a clear
232 defence response to both fungi (table S4). Enriched biological process GO terms among

233 shared downregulated genes included response to nitrate, nitrate transmembrane transport
234 and nitrate assimilation (figure 4D). Highly enriched molecular function GO terms among
235 upregulated genes included manganese ion binding, oxidoreductase activity and heme
236 binding. Highly enriched molecular function GO terms among downregulated genes included
237 nitrate transmembrane transporter activity and oxygen binding (table S5A). Highly enriched
238 cellular component GO terms among upregulated genes included extracellular region (table
239 S5B).

240 GO enrichment analysis was repeated for DEGs unique to the wheat response to *G.*
241 *hyphopodioides* at 5 dpi. Cinnamic acid metabolic process, glutathione metabolic process and
242 benzene-containing compound metabolic process were among the top 10 upregulated
243 biological process GO terms. In contrast, cell wall organisation or biogenesis, cell cycle and
244 anatomical structure morphogenesis were among the top 10 downregulated biological process
245 GO terms (figure 4E). Highly enriched molecular function GO terms among upregulated genes
246 included phenylalanine ammonia lyase (PAL) activity, glutathione transferase activity and ion
247 binding. In contrast, structural constituents of chromatin, tubulin binding and nucleosome
248 binding were highly enriched among the downregulated genes (table S6A). Highly enriched
249 cellular component function GO terms among downregulated genes included nucleosome,
250 microtubule cytoskeleton and protein-DNA complex (table S6B).

251

252 **Wheat phytohormone response to *G. hyphopodioides* colonisation and *G. tritici*** 253 **infection**

254 Regulation of the JA signalling pathway was identified as a newly upregulated GO term at 5
255 dpi in *G. hyphopodioides* colonised roots (see above). The GO term comprised 26 DEGs (out
256 of a total of 77 known genes in wheat), all of which were TIFY transcription factors. In contrast,
257 just three TIFY transcription factors (TIFY10C-like_TraesCS5D02G219300, TIFY10C-like
258 _TraesCS5B02G211000, TIFY11E-like_TraesCS7D02G204700) were DE in *G. tritici* infected
259 plants compared to the control. Although not identified by GO enrichment analysis, we also
260 investigated the expression of JA biosynthesis genes. In total, 23 JA biosynthesis-related
261 genes were DE (17 up/ 6 down) in response to *G. hyphopodioides* at 5 dpi. The list included
262 lipoxygenase (LOX), allene oxide synthase (AOS) and AOS-like, 12-oxophytodienoate
263 reductase (OPR) and OPR-like, and 3-ketoacyl-CoA thiolase (KAT-like) genes. Of these
264 genes, only one (LOX8_TraesCS7B02G145200) was differentially expressed in response to
265 *G. tritici* at 5 dpi (figure 5A, table S7).

266 The JA and ET signalling are often closely linked. Therefore, we investigated genes involved
267 in ET biosynthesis and signalling. Five ACC-oxidase (ACO-like) genes were upregulated in
268 response to *G. hyphopodioides* at 5 dpi. In addition, 22 ethylene responsive transcription
269 factor-like (ERF-like) genes, key integrators of downstream ET and JA signal transduction
270 pathways (Lorenzo et al., 2003), were DE (19 up/ 3 down) in response to *G. hyphopodioides*
271 by 5 dpi. In contrast, four ERF-like genes (TraesCS4A02G001300, TraesCS5B02G565400,
272 TraesCS1A02G231200, TraesCS1B02G231500) were upregulated at 4 dpi and two
273 (TraesCS5B02G565400, TraesCS1A02G231200) were upregulated at 5 dpi in *G. tritici*
274 infected roots compared to the control (figure 5B, table S7). Salicylic acid (SA) is another key
275 phytohormone involved in the plant response to pathogen invasion. SA signalling was not
276 identified as a significantly enriched GO term in response to *G. hyphopodioides* or *G. tritici* at
277 any time point.

278 To investigate whether the local transcriptional changes described above resulted in altered
279 hormone levels, hormone quantifications of JA and SA were carried out in *G. hyphopodioides*
280 colonised, *G. tritici* infected and uninoculated control roots at 5 dpi. We found no significant
281 difference in the levels of JA or SA between any treatments (figure 5C).

282

283 ***G. hyphopodioides* colonisation results in the early induction of lignin biosynthesis**
284 **genes**

285 PAL activity, essential for the lignin biosynthesis pathway, was identified as a significantly
286 enriched molecular function GO term in the unique wheat response to *G. hyphopodioides* at
287 5 dpi (see table S6A). To investigate root lignification in response to *G. hyphopodioides* and
288 *G. tritici*, we explored the expression of key genes involved in the lignin biosynthesis pathway
289 in wheat (figure 6A). *G. hyphopodioides* colonisation resulted in the earlier upregulation of
290 lignin biosynthesis genes compared to *G. tritici*, with key genes such as arogonate
291 dehydratase (ADT), phenylalanine ammonia-lyase (PAL), cinnamate 4-hydroxylase (4CL) and
292 cinnamoyl-CoA reductase (CCR) significantly upregulated at 4 dpi (figure 6B). However, two
293 of eight caffeic acid O-methyltransferase (COMT) genes detected were already significantly
294 upregulated in response to *G. tritici* at 2 dpi (TraesCS5D02G488800,
295 TraesCS5D02G488900). Interestingly, the remaining COMT genes (TraesCS2B02G066100,
296 TraesCSU02G024300, TraesCS3B02G612000, TraesCS7D02G539100,
297 TraesCS6D02G008200, TraesCS7D02G538900) were strongly downregulated in response to
298 *G. hyphopodioides* by 5 dpi, suggesting a decrease in the proportion of syringyl (S)-lignin.
299 Most striking however, was the significant upregulation of 37 PAL genes in response to *G.*
300 *hyphopodioides*, compared to the upregulation of just 12 PAL genes in response to *G. tritici* at
301 5 dpi (figure 6B, table S8).

302 To visualise lignification of infected root tissues, potassium permanganate staining was
303 performed on transverse sections of samples harvested at 5 dpi (figure 6C). The percentage
304 of total cell wall area with dark potassium permanganate staining (measured in ImageJ) was
305 used to quantify relative cell wall lignification. Based on these measurements, *G. tritici* infected
306 roots exhibited the highest levels of cell wall lignification, though both *G. hyphopodioides* and
307 *G. tritici* infection resulted in increased cell wall lignin levels compared to uninoculated control
308 roots at 5 dpi (figure 6D). Plant lignitubers, lignified callose deposits surrounding hyphal tips
309 (Bradshaw et al., 2020; Huang et al., 2001; Park et al., 2022), were often detected in cells
310 containing fungal hyphae, though these structures were more common in *G. tritici* infected
311 samples.

312

313 ***G. hyphopodioides* colonisation results in local downregulation of cell wall**
314 **organisation and biogenesis genes**

315 The biological process GO term “cell wall organisation and biogenesis” was identified as being
316 unique to the wheat response to *G. hyphopodioides* at 5 dpi (see figure 4E). In total, 124 genes
317 involved in cell wall organisation and biogenesis (out of 1122 total known genes involved in
318 cell wall organisation and biogenesis in wheat) were downregulated in response to *G.*
319 *hyphopodioides* at 5 dpi (table S9). In contrast, *G. tritici* infection did not lead to the differential
320 expression of any genes within the cell wall organisation and biogenesis GO term. Focussing
321 on the top 30 DE genes within this GO term in *G. hyphopodioides* colonised plants at 5 dpi,
322 we identified six xyloglucan endotransglycosylases/hydrolases (XTH) genes, three cellulose
323 synthase-like A-like (CSLA) genes, one cellulose synthase-like F (CSLF) gene and three
324 fasciclin-like arabinogalactan (FLA) genes (figure 7A). Though just one cellulose synthase-like
325 (CESA) gene was present in the list of top 30 DEGs, a total of 10 CESA genes were
326 downregulated at 5 dpi (table S9). To validate gene expression in the RNA-seq dataset, we
327 identified key cell-wall related genes where all three wheat homoeologues were
328 downregulated in *G. hyphopodioides* colonised plants relative to the mock inoculated controls
329 (figure 7B). RT-qPCR analyses of the selected targets revealed that, as expected, cell-wall
330 related genes CESA7-like, COBL-5D and FLA11 were significantly downregulated in *G.*
331 *hyphopodioides* colonised plants compared to the mock inoculated controls (figure 7C).

332 Discussion

333 The biocontrol potential of several non-pathogenic *Magnaporthaceae* species has been
334 reported as early as the 1970s (Deacon, 1973, 1976b; Wong & Southwell, 1980). However,
335 the precise mechanism(s) of control and the molecular pathways underpinning these
336 interactions have remained underexplored. In this study, we show that induced wheat
337 resistance mechanisms play a key role in *G. hyphopodioides*-mediated disease reduction.
338 Furthermore, we demonstrate that these resistance mechanisms operate at a local scale, with
339 effective disease protection conferred in roots pre-treated with *G. hyphopodioides*. However,
340 adding *G. hyphopodioides* after *G. tritici* resulted in increased take-all disease levels, thereby
341 posing a significant risk for field application. The potential for *G. hyphopodioides* to become
342 pathogenic in wheat and/or other cereal crops requires careful investigation. Nevertheless,
343 farmers may exploit the disease suppression ability of *G. hyphopodioides* by growing wheat
344 cultivars known to support natural populations, particularly when placed early in wheat
345 rotations (Osborne et al., 2018).

346 Though transcriptional studies into the *G. tritici*-wheat interaction have been carried out
347 previously for both host (Kang et al., 2019; Yang et al., 2015; Zhang et al., 2020) and pathogen
348 (Gazengel et al., 2020; Kang., 2019), this is not the case for the *G. hyphopodioides*-wheat
349 interaction. To investigate early wheat responses to *G. tritici* infection and uncover the local
350 wheat defence mechanisms responsible for *G. hyphopodioides*-induced disease control, we
351 performed comparative transcriptome profiling of *G. hyphopodioides* colonised and *G. tritici*
352 infected wheat using a precision inoculation method. Through detailed screening of infected
353 root material by confocal microscopy, we were able to characterise infection progression
354 across several time-points. In support of early studies into non-pathogenic *Magnaporthaceae*
355 species (Holden, 1976; Speakman & Lewis, 1978), we observed that while pathogenic *G. tritici*
356 grew into the vascular tissues of wheat at 5 dpi, growth of endophytic *G. hyphopodioides* was
357 always limited to the inner cortex. In addition, we observed the formation of *G. hyphopodioides*
358 SEVs in cortical cells at 5 dpi, while SEVs were not observed in *G. tritici* infected roots at any
359 time point. Interestingly, the formation of *G. hyphopodioides* SEVs at 5 dpi was concomitant
360 with a dramatic increase in the number of wheat DEGs. In contrast, the number of wheat DEGs
361 in *G. tritici* infected roots showed minimal increase between 4 dpi and 5 dpi.

362 TEM analysis of mature *G. hyphopodioides* SEVs revealed that SEVs share key similarities
363 with fungal resting structures such as chlamydospores, both being characterised by a
364 significantly thickened, multi-layered cell wall and an increased number of putative lipid bodies
365 (Francisco et al., 2019). Therefore, we hypothesise that *G. hyphopodioides* SEVs are fungal
366 resting structures which may be produced as a stress response to locally induced host
367 defences, as indicated by extensive transcriptional reprogramming at 5 dpi. Further
368 investigations are required to test this hypothesis and to determine what function, if any, SEVs
369 may play in fungal root infection. In contrast, *G. tritici* infections resulted in far fewer DEGs at
370 5 dpi (1074), the majority of which were upregulated. Interestingly, almost all DEGs identified
371 in response to *G. tritici* infection were also shared with the wheat response to *G.*
372 *hyphopodioides* colonisation. Despite triggering a significant wheat defence response, *G. tritici*
373 successfully causes disease, suggesting an ability to either suppress or overcome the local
374 wheat defences triggered. Therefore, future studies should focus on the elucidation of *G. tritici*
375 effectors, enzymes and secondary metabolites, which no doubt contribute to *G. tritici*
376 pathogenicity. One such effector, the ortholog of the barley powdery mildew effector gene
377 BEC1019, has already been associated with *G. tritici* virulence in wheat (Zhang et al., 2019).

378 Strikingly, 11% of all known cell wall organisation/biogenesis related genes in wheat were
379 downregulated in *G. hyphopodioides* colonised plants at 5 dpi, while none were significantly
380 downregulated in response to *G. tritici*. Impairment of cell wall integrity (CWI) by pathogen
381 invasion triggers the release of antimicrobial compounds and Damage-Associated Molecular
382 Patterns (DAMPs), the latter inducing plant innate immune responses upon recognition by

383 plant Pattern Recognition Receptors (PRRs) (Miedes et al., 2014). In this study, *G.*
384 *hyphopodioides* colonisation triggered the downregulation of 13 fasciclin-like
385 arabinogalactan (FLA) genes and 18 xyloglucan endotransglucosylase/hydrolase (XTH)
386 genes. FLA proteins contain a putative cell adhesion domain which may link the cell
387 membrane and the cell wall. FLA mutants in *Arabidopsis* exhibit a range of phenotypes
388 including reduced cellulose content, altered secondary cell-wall deposition and reduced
389 tensile strength (Ashagre et al., 2021). XTH genes are also involved in the maintenance of
390 CWI; these genes encode xyloglucan modifying enzymes which cleave xyloglucan chains to
391 enable cell wall expansion or alter cell wall strength (Cosgrove, 2005). In addition, we detected
392 the downregulation of 10 CESA genes. Though the exact mechanism is not yet known, a
393 number of studies in *Arabidopsis* indicate a link between CESA expression, CWI and disease
394 resistance. Mutations in the CESA4, CESA7 and CESA8 genes, required for secondary cell
395 wall formation in *Arabidopsis*, confer enhanced resistance to the necrotrophic fungus
396 *Plectosphaerella cucumerina* and the biotrophic bacterium *Ralstonia solanacearum*
397 (Hernández-Blanco et al., 2007). In addition, pathogenic *Fusarium oxysporum* root infection
398 of *Arabidopsis* results in the downregulation of various CESAs, causing an alteration in primary
399 cell wall cellulose and contributing to disease resistance (Menna et al., 2021). Furthermore,
400 mutations in CESA genes in *Arabidopsis* trigger the activation of defence responses and the
401 biosynthesis of lignin, regulated at least in part, by the jasmonic acid (JA) and ethylene (ET)
402 signalling pathways (Caño-Delgado et al., 2003). A link between JA/ET signalling and reduced
403 cellulose levels has also previously been reported by Ellis et al., (2002). Thus, our finding that
404 *G. hyphopodioides* colonisation results in the upregulation of lignin biosynthesis genes and
405 JA/ET signalling genes is pertinent.

406 Previous studies have reported higher levels of cell wall lignification in response to colonisation
407 by several non-pathogenic *Magnaporthaceae* species (Huang et al., 2001; Speakman &
408 Lewis, 1978). In the present study, we detected earlier and higher expression of lignin
409 biosynthesis genes in *G. hyphopodioides* colonised tissues compared to *G. tritici* infected
410 tissues. In contrast, local cell wall lignification (as determined by potassium permanganate
411 staining) was more prominent in *G. tritici* infected roots at 5 dpi. However, the downregulation
412 of several COMT genes in response to *G. hyphopodioides* is noteworthy. COMT genes are
413 involved in the synthesis of the S unit of lignin, and downregulation of these genes has a
414 minimal effect on total lignin content (Nguyen et al., 2016). Such changes in lignin composition
415 can drastically alter the outcome of plant-pathogen interactions (Höch et al., 2021; Ma et al.,
416 2018; Quentin et al., 2009). Therefore, despite contrasting results, cell wall lignification could
417 play an important role in *G. hyphopodioides*-mediated take-all control.

418 In our dataset, 26 TIFY TFs, involved in the cross-talk between JA and other phytohormones
419 (Singh & Mukhopadhyay, 2021) were upregulated in response to *G. hyphopodioides* at 5 dpi.
420 Just three TIFY TFs were significantly upregulated in response to *G. tritici*. In addition, *G.*
421 *hyphopodioides* colonisation resulted in the upregulation of a greater number of ERF-like
422 genes, known to integrate ET and JA signal transduction pathways (Lorenzo et al., 2003).
423 Phytohormone quantifications using ultra-high-performance liquid chromatography (UHPLC)
424 yielded highly variable results, and we did not detect a significant difference in local JA levels
425 between any treatment. However, high levels of variability may have been due to the transient
426 nature of local JA signalling in plants (Ruan et al., 2019). Thus, unlike in EMR by non-
427 pathogenic *Fusarium* species, *G. hyphopodioides*-induced resistance is potentially mediated,
428 at least to some extent, by the JA/ET signalling pathway. Further investigation is required to
429 determine whether the disruption of CWI mechanisms is directly responsible for the activation
430 of JA/ET mediated defence pathway and the lignin biosynthesis pathway. In addition, future
431 studies should investigate plant and fungal gene expression during *G. tritici* infection of roots
432 already colonised by *G. hyphopodioides*.

433 In summary, we demonstrate rapid and extensive transcriptional reprogramming in *G.*
434 *hyphopodioides* colonised wheat roots, characterised by the strong local induction of diverse
435 plant defence mechanisms. We propose that the collective effect of these local defence

436 mechanisms, particularly relating to cell-wall mediated resistance, are responsible for *G.*
437 *hyphopodioides*-mediated take-all control. Due to the lack of high-quality annotated *G. tritici*
438 and *G. hyphopodioides* genomes, comparative analysis of fungal gene expression during *G.*
439 *hyphopodioides* colonisation and *G. tritici* infection was not possible in this study. When
440 combined with the RNA-seq dataset presented here, future genome sequencing projects will
441 no doubt facilitate the investigation of novel *G. tritici* pathogenicity factors. In addition, further
442 analysis of non-pathogenic and pathogenic fungi within the diverse *Magnaporthaceae* family
443 may help to address wider questions relating to pathogen organ specificity, conserved fungal
444 root infection strategies and the determinants of fungal pathogenicity.

445

446 **Experimental Procedures**

447

448 **Fungal isolation and culture**

449 *G. hyphopodioides* (taxon id: 1940676) and *G. tritici* (taxon id: 36779) strains were isolated
450 from field soils at Rothamsted Farm using the soil baiting method (McMillan et al., 2011;
451 Osborne et al., 2018). Fungal isolates (see table 1), were maintained on potato dextrose agar
452 (PDA) plates at 21°C in the dark.

453

454 **Seedling infection pot assays and disease quantifications**

455 For seedling pot experiments, plastic pots (7.5 cm wide x 11 cm tall) were filled with damp
456 horticultural sand and ten untreated wheat seeds (cv. Hereward) were sown on the surface.
457 Seeds were covered with a thin layer of grit and pots were placed in a controlled environment
458 growth room for two weeks (16 hr day, light intensity 250 µmols, 15 °C day, 10 °C night). *G.*
459 *tritici* (isolate 16.NZ.1d) and *G. hyphopodioides* (isolate NZ.129.2C.17) inoculum was
460 prepared by placing ten fungal plugs (7 mm diameter) taken from the leading edge of each
461 colony into a 1 L flask containing 400 ml potato dextrose broth (PDB). Flasks were placed in
462 an orbital incubator for 7 days at 25 °C, 120 RPM. Liquid cultures were homogenised by
463 passing through a 2.8 mm sterile sieve. Homogenised cultures were diluted with sterile distilled
464 water in a 2:3 ratio. The first inoculum treatment was added into the pots after two weeks of
465 plant growth. Inoculum (50 ml) was poured directly onto the root system using a funnel inserted
466 into the sand. All seedlings were harvested three weeks after the final inoculum addition to
467 allow take-all disease symptoms to develop (see figure S7A). Five replicates were prepared
468 per treatment, and the experiment was repeated twice.

469 Visual disease assessments were carried out as previously described (McMillan et al., 2011)
470 and qPCR quantification of *G. tritici* fungal biomass was performed by targeting a 105-bp
471 partial DNA sequence of the translation elongation factor 1-alpha (EF1-α) gene, using primers
472 GtEFF1 (5'-CCCTGCAAGCTCTTCTTAG-3') and GtEFR1 (5'-
473 GCATGCGAGGTCCCAAAA-3') with the TaqMan probe (5'-6FAM-ACTGCACAGACCATC-
474 MGB-3') (Thermo Scientific™, USA) (Keenan et al., 2015).

475 For split-root experiments, roots from 2-week old wheat seedlings (cv. Chinese Spring) were
476 split across two pots (pot A, pot B) joined at one side. Pots were filled with sand and covered
477 with grit. Roots in pot A received *G. hyphopodioides* liquid inoculum (isolate NZ.129.2C.17),
478 using the method described above. Plants were left to grow for one week before inoculating
479 with *G. tritici* liquid inoculum (isolate 17LH(4)19d1). To investigate whether *G. hyphopodioides*
480 provides local control against take-all disease, *G. tritici* inoculum was added to *G.*
481 *hyphopodioides* colonised roots in pot A. To investigate whether *G. hyphopodioides* provides
482 systemic control against take-all disease, *G. tritici* inoculum was added to uninoculated roots

483 in pot B (see figure S7B). Plants were harvested three weeks later. Five replicates were
484 prepared per treatment, and the experiment was repeated three times.

485

486 **Plant growth, inoculation and root sampling for RNA sequencing and bioimaging**

487 A precision inoculation method was developed to enable the investigation of local plant
488 responses to fungal infection (see figure S8). Wheat seeds cv. Chinese Spring were surface
489 sterilised with 5% (v/v) sodium hypochlorite for five minutes and pre-germinated in a controlled
490 environment growth chamber cabinet (20 °C day, 16 °C night, 16 hr light cycle) for two days.
491 Three pre-germinated seeds were transplanted onto a square petri dish plate (12 cm x 12 cm)
492 containing 1.5 % (w/v) water agar. Five replicates were prepared for each treatment. Plates
493 were placed vertically in the growth cabinet. After four days, one root from each plant was
494 inoculated with a fungal plug (4 cm x 0.5 cm) cut from the leading edge of a 2-week old fungal
495 colony growing on 1.5 % water agar. Inoculated roots were sampled daily from 2-6 days post
496 inoculation (dpi). Briefly, two 1 cm root samples were harvested from the inoculated area on
497 each root and snap frozen in liquid nitrogen for RNA extraction. To determine the stage of
498 fungal colonisation in these harvested samples, 2 x 0.5 cm root pieces were sampled from the
499 areas directly above and below each sample. Root pieces were stored in 50% ethanol for
500 subsequent assessment by confocal microscopy.

501

502 **Fluorescent staining and confocal microscopy analyses**

503 To assess colonisation in whole root pieces, samples were cleared in 10% w/v potassium
504 hydroxide for 5 minutes at 70 °C, before staining with Propidium Iodide (PI) (10 µg/ml) and
505 Wheat Germ Agglutinin, Alexa Fluor™ 488 Conjugate (WGA) (10 µg/ml). To visualise vascular
506 infection by *G. tritici*, transversal root sections were cut by hand using a fine edged razor blade
507 under a dissecting microscope. Confocal microscopy was performed using a ZEISS 780
508 Confocal Laser Scanning Microscope (ZEISS, Germany). WGA fluorescence was excited at
509 495 nm and detected at 519 nm. PI fluorescence was excited at 535 nm and detected at 617
510 nm.

511

512 **RNA extraction**

513 Following confocal assessment (see above), root pieces (1 cm each) at the same stage of
514 fungal colonisation were pooled together to create a single sample for RNA extraction. Total
515 RNA was extracted from frozen root material using the E.Z.N.A.® Plant RNA Kit with the
516 associated RNase-free DNase I Set (Omega-Biotek, USA), following the standard protocol
517 provided. RNA quality was assessed based on the RNA Integrity Number (RIN), measured
518 using the Bioanalyser 2100 with the corresponding RNA 6000 Nano Kit (Agilent, USA), as per
519 manufacturer instructions.

520

521 **Library preparation and sequencing**

522 mRNA library preparation was carried out by Novogene (China) using the Novogene RNA
523 Library Prep Set (PT042) for polyA enrichment. Libraries were sequenced by Illumina
524 NovaSeq to generate 150 bp paired-end reads, with a target of 40 million paired-end reads
525 per sample.

526

527 **Transcriptome annotation and analysis**

528 Quality control of reads was performed using MultiQC (<https://multiqc.info/>). Sequence
529 trimming of recognised adaptors was performed using Trimmomatic where appropriate
530 (Bolger et al., 2014). Reads were mapped to the Chinese Spring (IWGSC RefSeq v2.1) (Zhu
531 et al., 2021) using HiSat2 (Kim et al., 2019). To ensure that fungal biomass was consistent
532 among replicates of the same treatment, reads were also mapped to the *G. tritici* genome
533 (Okagaki et al., 2015). Three samples were identified as outliers based on standardised
534 residuals of the percentage of reads mapped to *G. tritici*. Outliers were subsequently excluded
535 from further analyses (table S10). All treatments contained at least four biological replicates,
536 with the majority containing five biological replicates. Reads were not aligned to *G.*
537 *hyphopodioides* due to the lack of a high-quality genome. Count determination was performed
538 using FeatureCounts (Liao et al., 2014) on the R Bioconductor platform
539 (<https://bioconductor.org/>).

540 Library normalisation and differential expression (DE) calling was carried out using the
541 Bioconductor package DESeq2 (Love et al., 2014) in R studio. Gene expression levels were
542 compared between *G. tritici* infected and *G. hyphopodioides* colonised samples and the
543 uninoculated control samples for each time point individually. DE genes were identified by
544 applying a log₂ fold change filter of ≥ 1 or ≤ -1 . The DESeq2 implementation of Benjamini-
545 Hochberg (Benjamini & Hochberg, 1995) was used to control for multiple testing ($q < 0.05$).
546 Gene Ontology (GO) enrichment analysis was performed for significantly up- and down-
547 regulated wheat genes separately via <http://www.geneontology.org>, using the Panther
548 classification system.

549

550 **Statistical analyses**

551 Statistical analyses were done using Genstat 20th Edition (VSN International Ltd, Hemel
552 Hempstead, UK). Percentage disease data were analysed using a Generalised Linear
553 Regression Model (GLM) with a binomial distribution and LOGIT link function. Analyses were
554 adjusted for over-dispersion and treatment effects tested using deviance ratios (F-statistics)
555 when the residual mean deviance was greater than 1. Data were back-transformed from the
556 LOGIT scale (using the equation $\exp(x)/(1+\exp(x))$) for graphical presentation. For continuous
557 outcome variables such as plant biomass, data were analysed by Analysis of Variance
558 (ANOVA). Tukey's multiple comparisons test was carried out when more than one interaction
559 was of interest.

560

561 **Acknowledgements**

562 TC was supported by the Biotechnology and Biological Sciences Research Council (BBSRC)
563 funded University of Nottingham Doctoral Training Programme (BB/M008770/1). JPG, DS and
564 KHK were supported by the BBSRC Institute Strategic Programme (ISP) Grant, Designing
565 Future Wheat (BBS/E/C/00010250). In addition, DS is supported by the BBSRC ISP Grant
566 (BB/CCG2280/1) and KHK by the BBSRC ISP Grant, Delivering Sustainable Wheat
567 (BB/X011003/1 and BBS/E/RH/230001B). GC is supported by the defra funded Wheat
568 Genetic Improvement Network, WGIN (CH0109). VA is supported by the BBSRC funded
569 South West Biosciences Doctoral Training Partnership (BB/T008741/1).

570 We thank Smita Kurup and Hannah Walpole (Plant Sciences for the Bioeconomy, Rothamsted
571 Research) for advice and assistance with fluorescent staining and confocal microscopy of
572 wheat roots; Jess Hammond (Protecting Crops and the Environment, Rothamsted Research)
573 for help with fungal isolations and plant care; Matthew Dickinson (University of Nottingham)
574 for his feedback on the project.

575 **Data availability statement**

576 The data that support the findings of this study are openly available in the NCBI Gene
577 Expression Omnibus (GEO) at <https://www.ncbi.nlm.nih.gov/geo/>, reference number
578 GSE242417.

579

580 **References**

581 Ashagre, H., Zaltzman, D., Idan-Molakandov, A., Romano, H., Tzfadia, O., & Harpaz-Saad,
582 S. (2021). FASCICLIN-LIKE 18 Is a New Player Regulating Root Elongation in Arabidopsis
583 thaliana. *Frontiers in Plant Science*, 12, 391.
584 <https://doi.org/10.3389/FPLS.2021.645286/BIBTEX>

585 Asher, M. J. C., & Shipton, P. J. (1981). *Biology and control of take-all* (M. J. C. Asher & P. J.
586 Shipton, Eds.). London Academic Press.

587 Ban, Y., Tang, M., Chen, H., Xu, Z., Zhang, H., & Yang, Y. (2012). The Response of Dark
588 Septate Endophytes (DSE) to Heavy Metals in Pure Culture. *PLoS ONE*, 7(10).
589 <https://doi.org/10.1371/journal.pone.0047968>

590 Benjamini, Y., & Hochberg, Y. (1995). Controlling the False Discovery Rate: A Practical and
591 Powerful Approach to Multiple Testing. *Journal of the Royal Statistical Society: Series B*
592 (*Methodological*), 57(1), 289–300. <https://doi.org/10.1111/J.2517-6161.1995.TB02031.X>

593 Bolger, A. M., Lohse, M., & Usadel, B. (2014). Trimmomatic: A flexible trimmer for Illumina
594 sequence data. *Bioinformatics*, 30(15), 2114–2120.
595 <https://doi.org/10.1093/bioinformatics/btu170>

596 Boller, T., & Felix, G. (2009). A Renaissance of Elicitors: Perception of Microbe-Associated
597 Molecular Patterns and Danger Signals by Pattern-Recognition Receptors. *Annual Review of*
598 *Plant Biology*, 60(1), 379–406. <https://doi.org/10.1146/annurev.arplant.57.032905.105346>

599 Bradshaw, R. E., Bellgard, S. E., Black, A., Burns, B. R., Gerth, M. L., McDougal, R. L., Scott,
600 P. M., Waipara, N. W., Weir, B. S., Williams, N. M., Winkworth, R. C., Ashcroft, T., Bradley, E.
601 L., Dijkwel, P. P., Guo, Y., Lacey, R. F., Mesarich, C. H., Panda, P., & Horner, I. J. (2020).
602 *Phytophthora agathidicida*: research progress, cultural perspectives and knowledge gaps in
603 the control and management of kauri dieback in New Zealand. In *Plant Pathology* (Vol. 69,
604 Issue 1, pp. 3–16). Blackwell Publishing Ltd. <https://doi.org/10.1111/ppa.13104>

605 Caño-Delgado, A., Penfield, S., Smith, C., Catley, M., & Bevan, M. (2003). Reduced cellulose
606 synthesis invokes lignification and defense responses in *Arabidopsis thaliana*. *Plant Journal*,
607 *34*(3), 351–362. <https://doi.org/10.1046/j.1365-313X.2003.01729.x>

608 Cosgrove, D. J. (2005). Growth of the plant cell wall. *Nature Reviews Molecular Cell Biology*
609 *2005 6:11*, *6*(11), 850–861. <https://doi.org/10.1038/nrm1746>

610 de Lamo, F. J., & Takken, F. L. W. (2020). Biocontrol by *Fusarium oxysporum* Using
611 Endophyte-Mediated Resistance. *Frontiers in Plant Science*, *11*, 500488.
612 <https://doi.org/10.3389/FPLS.2020.00037/BIBTEX>

613 Deacon, J. W. (1973). *Phialophora radiculicola* and *Gaeumannomyces graminis* on roots of
614 grasses and cereals. *Transactions of the British Mycological Society*, *61*(3), 471–485.
615 [https://doi.org/10.1016/s0007-1536\(73\)80117-2](https://doi.org/10.1016/s0007-1536(73)80117-2)

616 Deacon, J. W. (1976a). Biology of the *Gaeumannomyces graminis* Arx & Olivier/*Phialophora*
617 *radiculicola* Cain Complex on Roots of the Gramineae. *EPPO Bulletin*, *6*(5), 349–363.
618 <https://doi.org/10.1111/j.1365-2338.1976.tb02033.x>

619 Deacon, J. W. (1976b). Biological control of the take-all fungus, *Gaeumannomyces graminis*,
620 by *Phialophora radiculicola* and similar fungi. *Soil Biology and Biochemistry*, *8*(4), 275–283.
621 [https://doi.org/10.1016/0038-0717\(76\)90057-2](https://doi.org/10.1016/0038-0717(76)90057-2)

622 Delgado-Baquerizo, M., Guerra, C. A., Cano-Díaz, C., Egidí, E., Wang, J. T., Eisenhauer, N.,
623 Singh, B. K., & Maestre, F. T. (2020). The proportion of soil-borne pathogens increases with
624 warming at the global scale. *Nature Climate Change*, *10*(6), 550–554.
625 <https://doi.org/10.1038/s41558-020-0759-3>

626 Dufresne, M., & Osbourn, A. E. (2001). Definition of Tissue-Specific and General
627 Requirements for Plant Infection in a Phytopathogenic Fungus. *Molecular Plant-Microbe*
628 *Interactions*, *14*(3), 300–307. <https://doi.org/10.1094/MPMI.2001.14.3.300>

629 Ellis, C., Karafyllidis, I., & Turner, J. G. (2002). Constitutive activation of jasmonate signaling
630 in an *Arabidopsis* mutant correlates with enhanced resistance to *Erysiphe cichoracearum*,
631 *Pseudomonas syringae*, and *Myzus persicae*. *Molecular Plant-Microbe Interactions*, *15*(10),
632 1025–1030. <https://doi.org/10.1094/MPMI.2002.15.10.1025>

633 Francisco, C. S., Ma, X., Zwysig, M. M., McDonald, B. A., & Palma-Guerrero, J. (2019).
634 Morphological changes in response to environmental stresses in the fungal plant pathogen

635 Zymoseptoria tritici. *Scientific Reports*, 9(1), 1–18. [https://doi.org/10.1038/s41598-019-45994-](https://doi.org/10.1038/s41598-019-45994-3)
636 3

637 Freeman, J., & Ward, E. (2004). Gaeumannomyces graminis, the take-all fungus and its
638 relatives. *Molecular Plant Pathology*, 5(4), 235–252. [https://doi.org/10.1111/j.1364-](https://doi.org/10.1111/j.1364-3703.2004.00226.x)
639 3703.2004.00226.x

640 Freeman, J., Ward, E., Gutteridge, R. J., & Bateman, G. L. (2005). Methods for studying
641 population structure, including sensitivity to the fungicide silthiofam, of the cereal take-all
642 fungus, Gaeumannomyces graminis var. tritici. *Plant Pathology*, 54(5), 686–698.
643 <https://doi.org/10.1111/j.1365-3059.2005.01252.x>

644 Gazengel, K., Lebreton, L., Lapalu, N., Amselem, J., Guillermin-Erckelboudt, A. Y., Tagu, D., &
645 Daval, S. (2020). pH effect on strain-specific transcriptomes of the take-all fungus. *PLoS ONE*,
646 15(7 July). <https://doi.org/10.1371/journal.pone.0236429>

647 Harris, J. M., Balint-Kurti, P., Bede, J. C., Day, B., Gold, S., Goss, E. M., Grenville-Briggs, L.
648 J., Jones, K. M., Wang, A., Wang, Y., Mitra, R. M., Sohn, K. H., & Alvarez, M. E. (2020). What
649 are the top 10 unanswered questions in molecular plant-microbe interactions? In *Molecular*
650 *Plant-Microbe Interactions* (Vol. 33, Issue 12, pp. 1354–1365). American Phytopathological
651 Society. <https://doi.org/10.1094/MPMI-08-20-0229-CR>

652 Henry Christopher, J. van R., & Van den Ende, W. (2018). UDP-glucose: A potential signaling
653 molecule in plants? *Frontiers in Plant Science*, 8, 2230.
654 <https://doi.org/10.3389/FPLS.2017.02230/BIBTEX>

655 Hernández-Blanco, C., Feng, D. X., Hu, J., Sánchez-Vallet, A., Deslandes, L., Llorente, F.,
656 Berrocal-Lobo, M., Keller, H., Barlet, X., Sánchez-Rodríguez, C., Anderson, L. K., Somerville,
657 S., Marco, Y., & Molinaa, A. (2007). Impairment of cellulose synthases required for
658 Arabidopsis secondary cell wall formation enhances disease resistance. *Plant Cell*, 19(3),
659 890–903. <https://doi.org/10.1105/tpc.106.048058>

660 Hernández-Restrepo, M., Groenewald, J. Z., Elliott, M. L., Canning, G., McMillan, V. E., &
661 Crous, P. W. (2016). Take-all or nothing. *Studies in Mycology*, 83, 19–48.
662 <https://doi.org/10.1016/j.simyco.2016.06.002>

663 Holden, J. (1976). Infection of wheat seminal roots by varieties of Phialophora radicola and
664 Gaeumannomyces graminis. *Soil Biology and Biochemistry*, 8(2), 109–119.
665 [https://doi.org/10.1016/0038-0717\(76\)90074-2](https://doi.org/10.1016/0038-0717(76)90074-2)

- 666 Huang, L., Kang, Z., & Buchenauer, H. (2001). Comparison of infection of wheat roots by
667 *Phialophora graminicola* and *Gaeumannomyces graminis* var. *tritici* by ultrastructural and
668 cytochemical studies. *Journal of Plant Diseases and Protection*, 108(6), 593–607.
- 669 Jones, J. D. G., & Dangl, J. L. (2006). The plant immune system. *Nature*, 444(7117), 323–
670 329. <https://doi.org/10.1038/nature05286>
- 671 Kang, X., Guo, Y., Leng, S., Xiao, L., Wang, L., Xue, Y., & Liu, C. (2019). Comparative
672 Transcriptome Profiling of *Gaeumannomyces graminis* var. *tritici* in Wheat Roots in the
673 Absence and Presence of Biocontrol *Bacillus velezensis* CC09. *Frontiers in Microbiology*,
674 10(1474). <https://doi.org/10.3389/fmicb.2019.01474>
- 675 Kang, X., Wang, L., Guo, Y., Zain Ul Arifeen, M., Cai, X., Xue, Y., Bu, Y., Wang, G., & Liu, C.
676 (2019). A Comparative Transcriptomic and Proteomic Analysis of Hexaploid Wheat's
677 Responses to Colonization by *Bacillus velezensis* and *Gaeumannomyces graminis*, Both
678 Separately and Combined. *Molecular Plant-Microbe Interactions*, 32(10).
679 <https://doi.org/10.1094/MPMI-03-19-0066-R>
- 680 Keenan, S., Cromey, M. G., Harrow, S. A., Bithell, S. L., Butler, R. C., Beard, S. S., & Pitman,
681 A. R. (2015). Quantitative PCR to detect *Gaeumannomyces graminis* var. *tritici* in symptomatic
682 and non-symptomatic wheat roots. *Australasian Plant Pathology*, 44(6), 591–597.
683 <https://doi.org/10.1007/s13313-015-0379-y>
- 684 Kim, D., Paggi, J. M., Park, C., Bennett, C., & Salzberg, S. L. (2019). Graph-based genome
685 alignment and genotyping with HISAT2 and HISAT-genotype. *Nature Biotechnology*, 37(8),
686 907–915. <https://doi.org/10.1038/s41587-019-0201-4>
- 687 Knapp, D. G., Németh, J. B., Barry, K., Hainaut, M., Henrissat, B., Johnson, J., Kuo, A., Lim,
688 J. H. P., Lipzen, A., Nolan, M., Ohm, R. A., Tamás, L., Grigoriev, I. V., Spatafora, J. W., Nagy,
689 L. G., & Kovács, G. M. (2018). Comparative genomics provides insights into the lifestyle and
690 reveals functional heterogeneity of dark septate endophytic fungi. *Scientific Reports*, 8(1), 1–
691 13. <https://doi.org/10.1038/s41598-018-24686-4>
- 692 Lee, W.-S., Rudd, J. J., Hammond-Kosack, K. E., & Kanyuka, K. (2014). *Mycosphaerella*
693 *graminicola* LysM Effector-Mediated Stealth Pathogenesis Subverts Recognition Through
694 Both CERK1 and CEBiP Homologues in Wheat. *C*, 27(3), 236–243.
695 <https://doi.org/10.1094/MPMI-07-13-0201-R>

- 696 Liao, Y., Smyth, G. K., & Shi, W. (2014). FeatureCounts: An efficient general purpose program
697 for assigning sequence reads to genomic features. *Bioinformatics*, 30(7), 923–930.
698 <https://doi.org/10.1093/bioinformatics/btt656>
- 699 Livak, K. J., & Schmittgen, T. D. (2001). Analysis of Relative Gene Expression Data Using
700 Real-Time Quantitative PCR and the 2- $\Delta\Delta$ CT Method. *Methods*, 25(4), 402–408.
701 <https://doi.org/10.1006/METH.2001.1262>
- 702 Lorenzo, O., Piqueras, R., Sánchez-Serrano, J. J., & Solano, R. (2003). ETHYLENE
703 RESPONSE FACTOR1 Integrates Signals from Ethylene and Jasmonate Pathways in Plant
704 Defense. *The Plant Cell*, 15(1), 165–178. <https://doi.org/10.1105/TPC.007468>
- 705 Love, M. I., Huber, W., & Anders, S. (2014). Moderated estimation of fold change and
706 dispersion for RNA-seq data with DESeq2. *Genome Biology*, 15(12), 550.
707 <https://doi.org/10.1186/s13059-014-0550-8>
- 708 Marcel, S., Paszkowski, U., Sawers, R., Oakeley, E., & Angliker, H. (2010). Tissue-adapted
709 invasion strategies of the rice blast fungus *Magnaporthe oryzae*. *Plant Cell*, 22(9), 3177–3187.
710 <https://doi.org/10.1105/tpc.110.078048>
- 711 McMillan, V. E., Hammond-Kosack, K. E., & Gutteridge, R. J. (2011). Evidence that wheat
712 cultivars differ in their ability to build up inoculum of the take-all fungus, *Gaeumannomyces*
713 *graminis* var. *tritici*, under a first wheat crop. *Plant Pathology*. [https://doi.org/10.1111/j.1365-](https://doi.org/10.1111/j.1365-3059.2010.02375.x)
714 [3059.2010.02375.x](https://doi.org/10.1111/j.1365-3059.2010.02375.x)
- 715 Menna, A., Dora, S., Sancho-Andrés, G., Kashyap, A., Meena, M. K., Sklodowski, K.,
716 Gasperini, D., Coll, N. S., & Sánchez-Rodríguez, C. (2021). A primary cell wall cellulose-
717 dependent defense mechanism against vascular pathogens revealed by time-resolved dual
718 transcriptomics. *BMC Biology*, 19(1), 1–20. <https://doi.org/10.1186/s12915-021-01100-6>
- 719 Miedes, E., Vanholme, R., Boerjan, W., & Molina, A. (2014). The role of the secondary cell
720 wall in plant resistance to pathogens. *Frontiers in Plant Science*, 5(358).
721 <https://doi.org/10.3389/fpls.2014.00358>
- 722 Nguyen, T. N., Son, S. H., Jordan, M. C., Levin, D. B., & Ayele, B. T. (2016). Lignin
723 biosynthesis in wheat (*Triticum aestivum* L.): Its response to waterlogging and association with
724 hormonal levels. *BMC Plant Biology*, 16(1). <https://doi.org/10.1186/s12870-016-0717-4>
- 725 Okagaki, L. H., Nunes, C. C., Sailsbery, J., Clay, B., Brown, D., John, T., Oh, Y., Young, N.,
726 Fitzgerald, M., Haas, B. J., Zeng, Q., Young, S., Adiconis, X., Fan, L., Levin, J. Z., Mitchell, T.

- 727 K., Okubara, P. A., Farman, M. L., Kohn, L. M., ... Dean, R. A. (2015). *Genome Sequences*
728 *of Three Phytopathogenic Species of the Magnaporthaceae Family of Fungi.*
729 <https://doi.org/10.1534/g3.115.020057>
- 730 Osborne, S. J., McMillan, V. E., White, R., & Hammond-Kosack, K. E. (2018). Elite UK winter
731 wheat cultivars differ in their ability to support the colonization of beneficial root-infecting fungi.
732 *Journal of Experimental Botany*, 69(12), 3103–3115. <https://doi.org/10.1093/jxb/ery136>
- 733 Palma-Guerrero, J., Chancellor, T., Spong, J., Canning, G., Hammond, J., McMillan, V. E., &
734 Hammond-Kosack, K. E. (2021). Take-All Disease: New Insights into an Important Wheat Root
735 Pathogen. *Trends in Plant Science*, 26(8), 836–848.
736 <https://doi.org/10.1016/j.tplants.2021.02.009>
- 737 Park, J. R., Kim, E. G., Jang, Y. H., Yun, B. J., & Kim, K. M. (2022). Selection strategy for
738 damping-off resistance gene by biotechnology in rice plant. *Plant and Soil*, 474(1–2), 277–
739 296. <https://doi.org/10.1007/s11104-022-05334-3>
- 740 Pok, B., Ngou, M., Ding, P., & Jones, J. D. G. (2022). Thirty years of resistance: Zig-zag
741 through the plant immune system. *The Plant Cell*. <https://doi.org/10.1093/PLCELL/KOAC041>
- 742 Reynolds, E. S. (1963). The use of lead citrate at high pH as an electron-opaque stain in
743 electron microscopy. *The Journal of Cell Biology*, 17(1), 208.
744 <https://doi.org/10.1083/JCB.17.1.208>
- 745 Ruan, J., Zhou, Y., Zhou, M., Yan, J., Khurshid, M., Weng, W., Cheng, J., & Zhang, K. (2019).
746 Jasmonic acid signaling pathway in plants. In *International Journal of Molecular Sciences* (Vol.
747 20, Issue 10). MDPI AG. <https://doi.org/10.3390/ijms20102479>
- 748 Singh, P., & Mukhopadhyay, K. (2021). Comprehensive molecular dissection of TIFY
749 Transcription factors reveal their dynamic responses to biotic and abiotic stress in wheat
750 (*Triticum aestivum* L.). *Scientific Reports*, 11(1), 1–17. [https://doi.org/10.1038/s41598-021-](https://doi.org/10.1038/s41598-021-87722-w)
751 [87722-w](https://doi.org/10.1038/s41598-021-87722-w)
- 752 Speakman, J. B., & Lewis, B. G. (1978). Limitation of *Gaeumannomyces graminis* by wheat
753 root responses to *Phialophora radicularis*. *New Phytologist*, 80(2), 373–380.
754 <https://doi.org/10.1111/j.1469-8137.1978.tb01571.x>
- 755 Su, Z. Z., Mao, L. J., Li, N., Feng, X. X., Yuan, Z. L., Wang, L. W., Lin, F. C., & Zhang, C. L.
756 (2013). Evidence for Biotrophic Lifestyle and Biocontrol Potential of Dark Septate Endophyte

757 Harpophora oryzae to Rice Blast Disease. *PLOS ONE*, 8(4), 61332.
758 <https://doi.org/10.1371/JOURNAL.PONE.0061332>

759 Thoms, D., Liang, Y., & Haney, C. H. (2021). Maintaining symbiotic homeostasis: How do
760 plants engage with beneficial microorganisms while at the same time restricting pathogens?
761 In *Molecular Plant-Microbe Interactions* (Vol. 34, Issue 5, pp. 462–469). American
762 Phytopathological Society. <https://doi.org/10.1094/MPMI-11-20-0318-FI>

763 Ulrich, K., Augustin, C., & Werner, A. (2000). Identification and characterization of a new group
764 of root-colonizing fungi within the Gaeumannomyces-Phialophora complex. *New Phytologist*,
765 145(1), 127–135. <https://doi.org/10.1046/j.1469-8137.2000.00553.x>

766 Ward, E., & Bateman, G. L. (1999). Comparison of Gaeumannomyces- and Phialophora-like
767 fungal pathogens from maize and other plants using DNA methods. *New Phytologist*, 141(2),
768 323–331. <https://doi.org/10.1046/j.1469-8137.1999.00346.x>

769 Wong, P. T. W., Mead, J. A., & Holley, M. P. (1996). Enhanced field control of wheat take-all
770 using cold tolerant isolates of Gaeumannomyces graminis var. graminis and Phialophora sp.
771 (lobed hyphopodia). *Plant Pathology*, 45(2), 285–293. <https://doi.org/10.1046/j.1365-3059.1996.d01-132.x>

773 Wong, P. T. W., & Southwell, R. J. (1980). Field control of take-all of wheat by avirulent fungi.
774 *Annals of Applied Biology*, 94(1), 41–49. <https://doi.org/10.1111/j.1744-7348.1980.tb03894.x>

775 Yang, L., Xie, L., Xue, B., Goodwin, P. H., Quan, X., Zheng, C., Liu, T., Lei, Z., Yang, X., Chao,
776 Y., & Wu, C. (2015). Comparative Transcriptome Profiling of the Early Infection of Wheat
777 Roots by Gaeumannomyces graminis var. tritici. *PLOS ONE*, 10(4), e0120691.
778 <https://doi.org/10.1371/journal.pone.0120691>

779 Zaninotto, F., Camera, S. La, Polverari, A., & Delledonne, M. (2006). Cross Talk between
780 Reactive Nitrogen and Oxygen Species during the Hypersensitive Disease Resistance
781 Response. *Plant Physiology*, 141(2), 379–383. <https://doi.org/10.1104/PP.106.078857>

782 Zhang, Y., Xu, K., Yu, D., Liu, Z., Peng, C., Li, X., Zhang, J., Dong, Y., Zhang, Y., Tian, P.,
783 Guo, T., & Li, C. (2019). The highly conserved barley powdery mildew effector BEC1019
784 confers susceptibility to biotrophic and necrotrophic pathogens in wheat. *International Journal*
785 *of Molecular Sciences*, 20(18), 1–16. <https://doi.org/10.3390/ijms20184376>

786 Zhang, J., Yan, H., Xia, M., Han, X., Xie, L., Goodwin, P. H., Quan, X., Sun, R., Wu, C., &
787 Yang, L. (2020). Wheat root transcriptional responses against Gaeumannomyces graminis

788 var . tritici. *Phytopathology Research*, 2(23). [https://doi.org/https://doi.org/10.1186/s42483-](https://doi.org/https://doi.org/10.1186/s42483-789-020-00066-7)

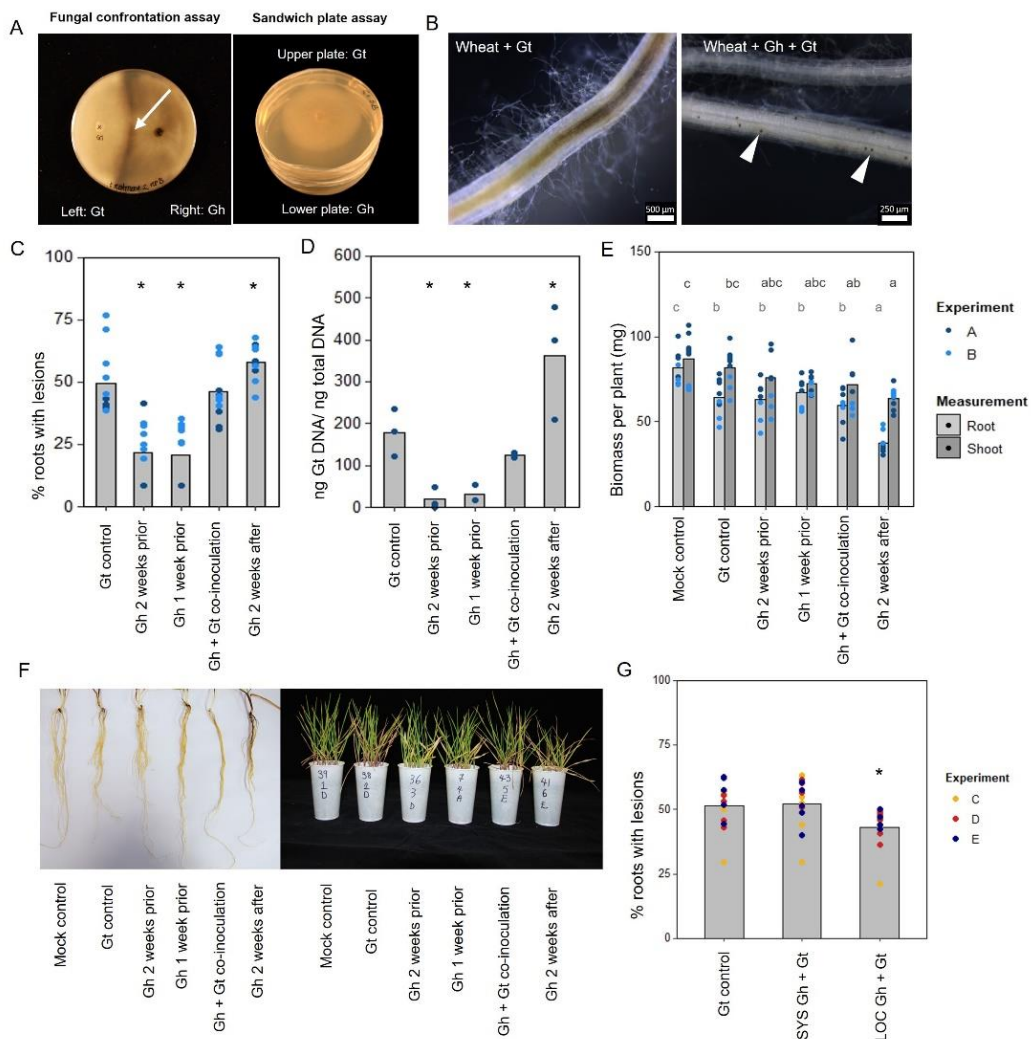
790 Zhou, F., Emonet, A., Déneraud Tendon, V., Marhavy, P., Wu, D., Lahaye, T., & Geldner, N.
791 (2020). Co-incidence of Damage and Microbial Patterns Controls Localized Immune
792 Responses in Roots. *Cell*, 180(3), 440–453. <https://doi.org/10.1016/j.cell.2020.01.013>

793 Zhu, T., Wang, L., Rimbart, H., Rodriguez, J. C., Deal, K. R., De Oliveira, R., Choulet, F.,
794 Keeble-Gagnère, G., Tibbits, J., Rogers, J., Eversole, K., Appels, R., Gu, Y. Q., Mascher, M.,
795 Dvorak, J., & Luo, M. C. (2021). Optical maps refine the bread wheat *Triticum aestivum* cv.
796 Chinese Spring genome assembly. *The Plant Journal*, 107(1), 303–314.
797 <https://doi.org/10.1111/TPJ.15289>

798

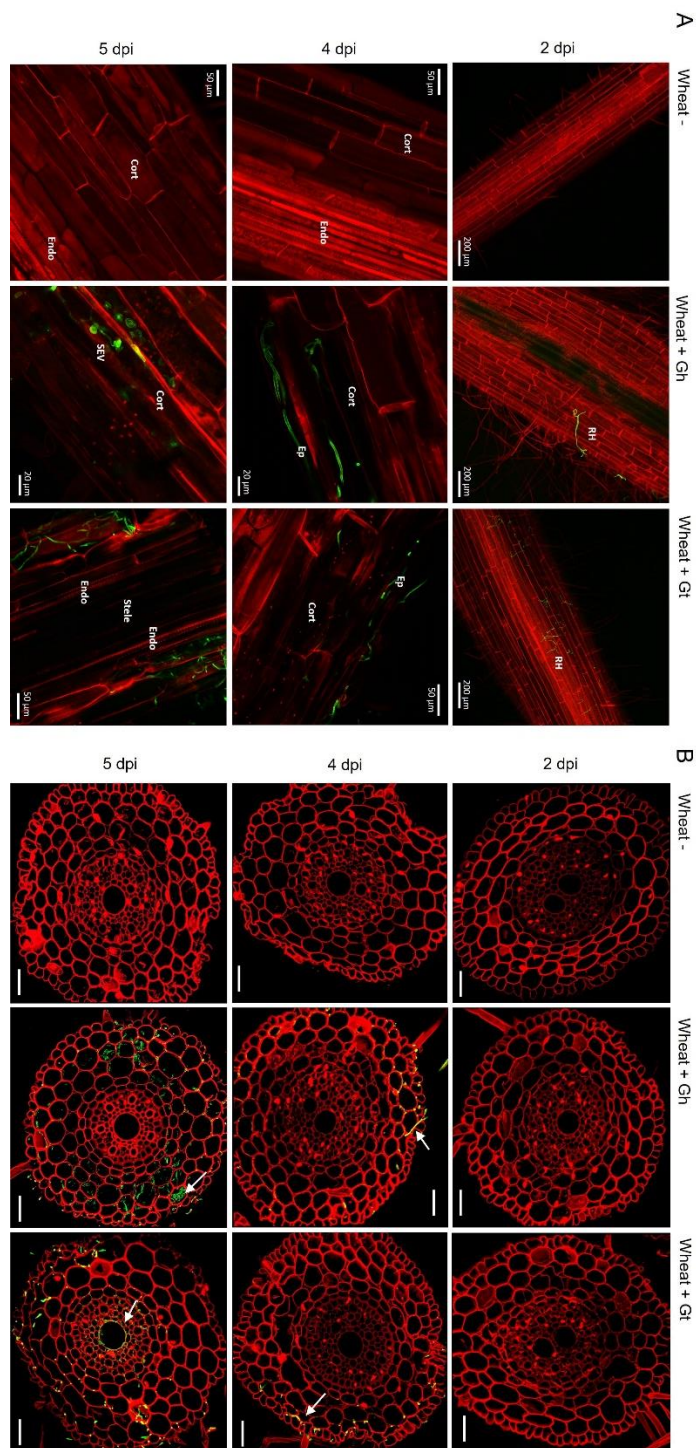
799 **Table 1.** Full list of Rothamsted fungal isolates used in the present study.

Isolate name	Year isolated	Rothamsted field name	Plot species, cultivar	ITS identification	species	Experiment
NZ.129.2C.17	2016	New Zealand	<i>T. aestivum</i> , Scout	<i>G. hyphopodioides</i>		Seedling pot infection assays, Split-root experiment, Fungal confrontation assay
63B-1	2018	Delafield	<i>T. aestivum</i> , Avalon	<i>G. hyphopodioides</i>		Fungal confrontation assay
NZ.24.2A.15	2015	New Zealand	<i>T. aestivum</i> , KWS Kielder	<i>G. hyphopodioides</i>		Fungal confrontation assay
S.03.13	2013	Summerdells I	<i>T. aestivum</i> , Conqueror	<i>G. hyphopodioides</i>		Fungal confrontation assay
P.09.13	2013	Pastures	<i>T. aestivum</i> , Conqueror	<i>G. hyphopodioides</i>		Fungal confrontation assay
105C-1	2018	Delafield	<i>T. aestivum</i> , Cadanza	<i>G. hyphopodioides</i>		Fungal confrontation assay
P.10.13	2013	Pastures	<i>T. aestivum</i> , Conqueror	<i>G. hyphopodioides</i>		Fungal confrontation assay
16.NZ.1d	2016	New Zealand	<i>T. aestivum</i> , Hereford	<i>G. tritici</i>		Seedling pot infection assays, Split-root experiment, Fungal confrontation assay
17LH(4)19d1	2017	Long Hoos	<i>T. aestivum</i> , Cadanza	<i>G. tritici</i>		Seedling pot infection assays, Split-root experiment, Fungal confrontation assay
Gt 17LH(4)8d	2017	Long Hoos	<i>T. aestivum</i> , Hereward	<i>G. tritici</i>		Fungal confrontation assay
Gt 17LH(4)9d2	2017	Long Hoos	<i>T. aestivum</i> , unknown	<i>G. tritici</i>		Fungal confrontation assay
Gt 17LH(4)23d	2017	Long Hoos	<i>T. aestivum</i> , Cadanza	<i>G. tritici</i>		Fungal confrontation assay
Gt 17LH(4)4e	2017	Long Hoos	<i>T. aestivum</i> , Hereward	<i>G. tritici</i>		Fungal confrontation assay



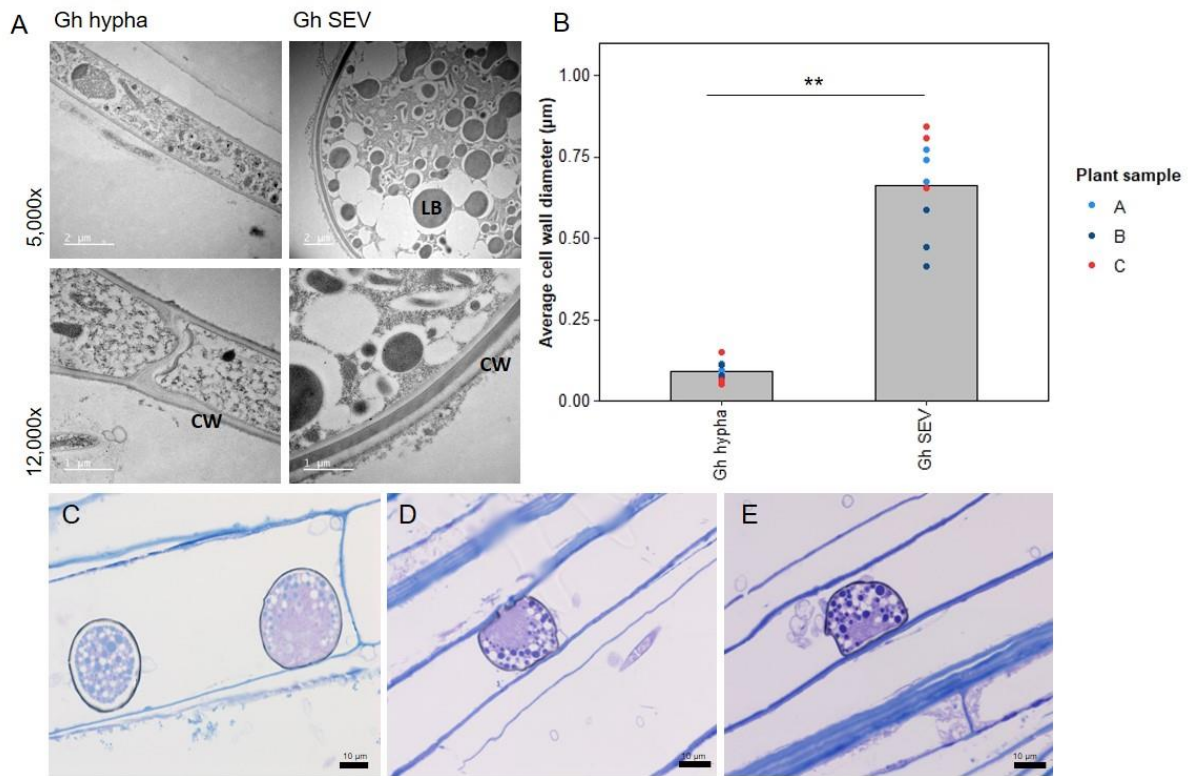
800

801 **Figure 1. *In vitro* and *in planta* interaction studies involving endophytic *G.***
 802 ***hyphopodioides* and pathogenic *G. tritici*.** A. *In vitro* fungal interaction assays on PDA
 803 plates. Fungal confrontation assays imaged 2 days following hyphal interaction, colonies in
 804 sandwich plate assays imaged 6 days after establishment. Arrow indicates a dark barrage in
 805 the interaction zone; B. Stereomicroscope images of wheat roots infected with *G. tritici* only,
 806 or co-inoculated with *G. hyphopodioides*. Arrowheads indicate *G. hyphopodioides* sub-
 807 epidermal vesicles (SEVs); C. Percentage of wheat roots (cv. Hereward) with take-all root
 808 lesions in co-inoculation experiments with *G. hyphopodioides* (GLM: $F=25.99$, d.f. 4, 49, p
 809 <0.001); D. *G. tritici* fungal biomass (ng *G. tritici* DNA/ ng total DNA) in co-inoculation
 810 experiments with *G. hyphopodioides*, as quantified by qPCR ($F=61.10$, d.f. 4, 38, $p<0.001$); E.
 811 Shoot and root dry biomass (mg) in *G. tritici* co-inoculation experiments with *G.*
 812 *hyphopodioides* ($F=6.49$, d.f. 5, 36, $p<0.001$; $F=4.50$, d.f. 5, 36, $p<0.01$, respectively); F.
 813 Representative images of wheat roots (left) and shoots (right) in co-inoculation experiments;
 814 G. The percentage of wheat roots (cv. Chinese Spring) with take-all lesions in split root co-
 815 inoculation experiments with *G. hyphopodioides* ($F=29.44$, d.f. 2, 36, $p=0.007$). Asterisks
 816 indicate a significant difference to the *G. tritici* control as calculated by Dunnett's post-hoc test
 817 ($p<0.05$). Letters indicate significant differences as calculated by Tukey's multiple
 818 comparisons test ($p<0.05$). Gt= *G. tritici*, Gh= *G. hyphopodioides*, SYS=systemic, LOC=local.



819

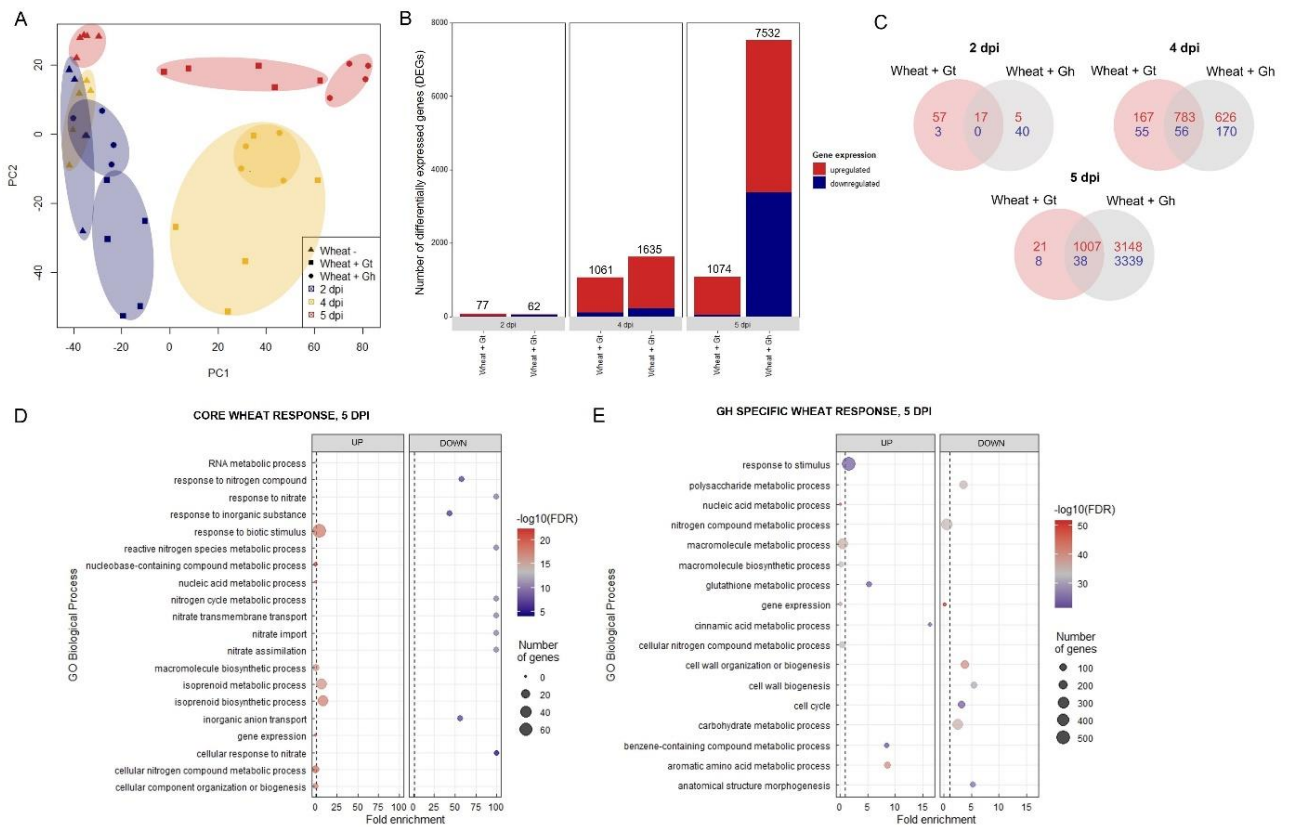
820 **Figure 2. Fluorescence images obtained by confocal microscopy of mock inoculated,**
 821 ***G. hyphopodioides* colonised or *G. tritici* infected wheat roots.** A. Confocal micrographs
 822 of whole root pieces highlighting fungal infection structures; B. Z- stack images of transversal
 823 sections showing colonisation of different root cell layers across time points. Gt= *G. tritici*, Gh=
 824 *G. hyphopodioides*, RH= runner hyphae, Ep= epidermal cell, Cort= cortical cell, SEV=
 825 subepidermal vesicle, Endo= endodermal barrier. Fungal hyphae (green) are stained with
 826 WGA-AF488, plant cell-walls (red) are stained with propidium iodide. White arrows in panel B
 827 indicate fungal hyphae. Scale bars in panel B represent 50 μm.



828

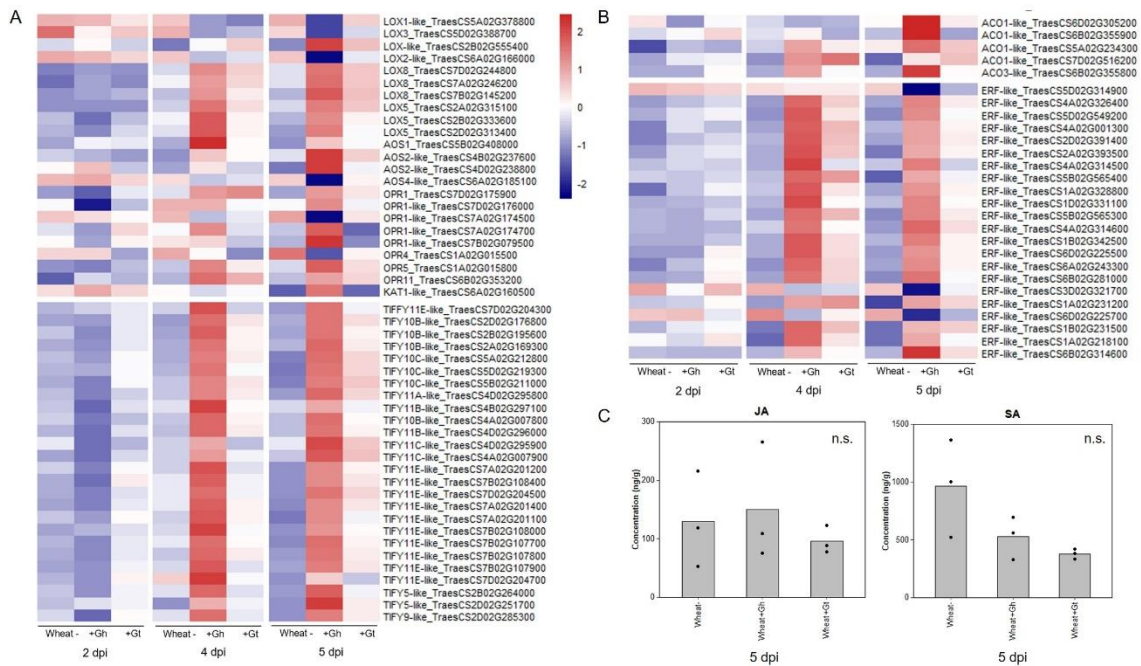
829 **Figure 3. Subepidermal vesicles (SEVs) produced by *G. hyphopodioides* (Gh) in wheat**
 830 **roots.** A. Transmission electron micrographs (TEM) of *Gh* hyphae (left) and SEVs (right); B.
 831 Average cell wall diameter (µm) of *Gh* fungal structures (F= 8.3, d.f. 2, 12, p<0.01); C- E. Light
 832 micrographs of *Gh* SEVs in semi-thin sections, stained with toluidine blue. CW=plant cell wall;
 833 LB=putative lipid body.

834



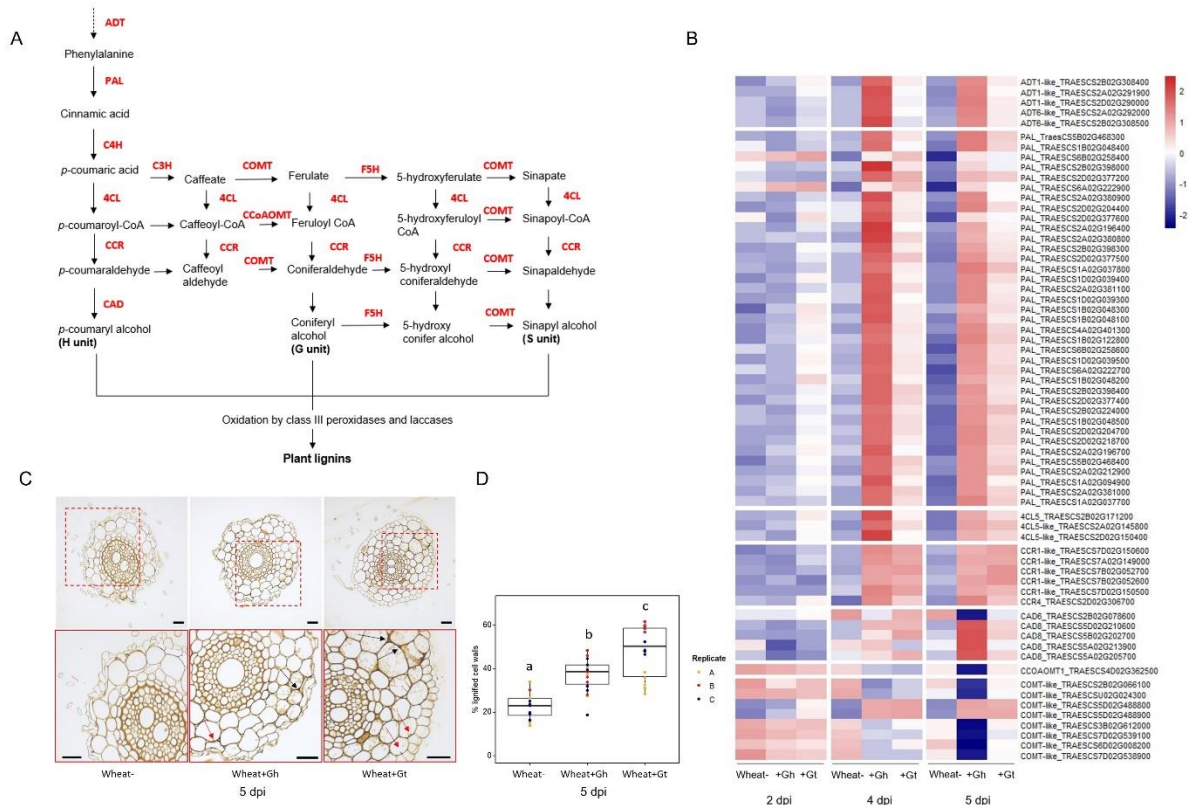
835

836 **Figure 4. Transcriptional profiling of *G. hyphopodioides* colonised or *G. tritici* infected**
 837 **wheat roots.** A. Principal Component Analysis (PCA) plot of sample distances based on
 838 transformed (variance stabilising transformation) gene count data. Data points have been
 839 categorised by shape and colour to denote treatment and time point, respectively; B. The
 840 number of differentially expressed genes (DEGs) in wheat colonised by *G. hyphopodioides* or
 841 *G. tritici* compared to uninoculated control samples; C. Venn diagram highlighting the number
 842 of unique and shared wheat DEGs in *G. tritici* infected or *G. hyphopodioides* colonised
 843 samples compared to the uninoculated control samples; D. Top 10 enriched biological process
 844 GO terms among DEGs in the shared wheat response to both *G. tritici* and *G. hyphopodioides*
 845 at 5 dpi; E. Top 10 enriched biological process GO terms unique to the wheat response to *G.*
 846 *hyphopodioides* colonisation at 5 dpi. The top 10 GO terms were determined by false
 847 discovery rate (FDR).



848

849 **Figure 5. Wheat phytohormone-associated gene responses and JA quantification in**
 850 **response to *G. hyphopodioides* (Gh) colonisation or *G. tritici* (Gt) infection. A.**
 851 **Expression of genes involved in the biosynthesis of JA and the regulation of the JA mediated**
 852 **signalling pathway; B. Expression of genes involved in ET biosynthesis and downstream ET**
 853 **signalling pathways. Heatmap data represent LOG transformed normalised genes counts; C.**
 854 **Phytohormone quantification of JA and SA in roots harvested at 5 dpi (F=0.30, d.f. 2, 6, p=**
 855 **0.75; F=4.19, d.f. 2, 6, p=0.07, respectively). n.s.= not significant. Data have been back-**
 856 **transformed from a square root scale. ACO, 1-aminocyclopropane-1-carboxylic acid oxidase;**
 857 **AOC, allene oxide cyclase; AOS, allene oxide synthase; ERF, ethylene responsive**
 858 **transcription factor; KAT, 3-ketoacyl-CoA thiolase; LOX, lipoxygenase; OPR, 12-**
 859 **oxophytodienoate reductase; TIFY, TIFY-domain containing transcription factor.**

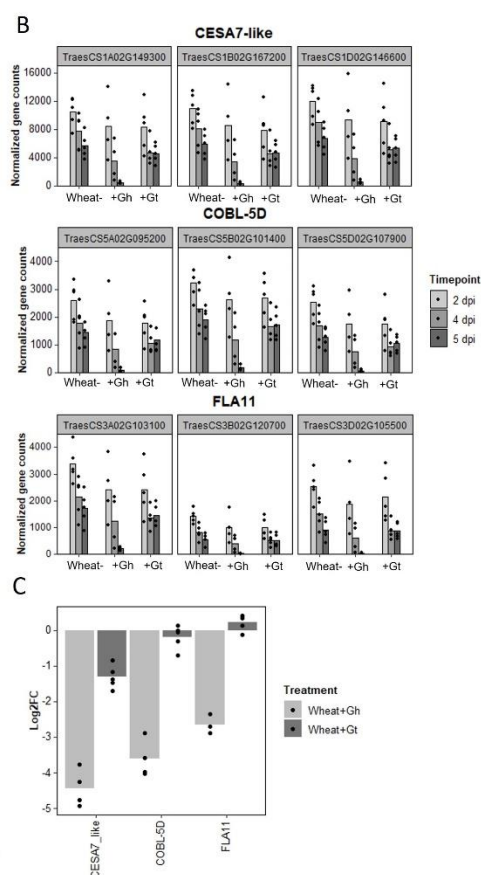


860

861 **Figure 6. Lignin biosynthesis pathway and the lignin responses to *G. hyphopodioides***
 862 **colonisation or *G. tritici* infection.** A. Schematic of the lignin biosynthesis pathway in plants
 863 (adapted from Nguyen et al., 2016); B. Expression of key genes involved in the lignin
 864 biosynthesis pathway, based on LOG transformed normalised gene counts; C. Micrographs
 865 of transversal root sections stained with potassium permanganate for the visualisation of cell
 866 wall lignification in response to fungal infection at 5 dpi. Black arrows indicate lignified cell wall
 867 thickenings, red arrows indicate plant lignitubers. Scale bars represent 50 μm ; D. Mean
 868 percentage of total cell wall area stained within dark parameters, indicating relative cell wall
 869 lignification ($F=34.61$, d.f. 2, 50, $p<.001$). Lowercase letters indicate Tukey post-hoc
 870 groupings. ADT, Arogenate dehydratase; PAL, phenylalanine ammonia-lyase; C4H,
 871 cinnamate 4-hydroxylase; 4CL, 4-coumarate CoA ligase; HCT, quinate shikimate *p*-
 872 hydroxycinnamoyltransferase; C3'H, *p*-coumaroylshikimate 3'-hydroxylase; CCoAOMT,
 873 caffeoyl-CoA O-methyltransferase; CCR, cinnamoyl-CoA reductase; F5H, ferulate 5-
 874 hydroxylase; CAD, cinnamyl alcohol dehydrogenase; COMT, caffeic acid O-
 875 methyltransferase.

A

Gene ID	Gene name	Log2FC	padj
TraesCS5A02G548500	XTH	-5.66	4.27E-22
TraesCS7A02G363000	XTH	-4.52	1.51E-17
TraesCS7D02G360100	XTH	-5.10	2.71E-10
TraesCS7D02G294300	CSLF6	-3.49	4.39E-10
TraesCS4B02G383000	XTH	-3.39	4.97E-10
TraesCS4D02G358700	XTH	-3.81	5.00E-10
TraesCS7B02G265000	XTH	-6.31	5.28E-10
TraesCS6A02G169200	CSLA1-like	-4.05	6.71E-09
TraesCS6B02G197200	CSLA1-like	-3.61	7.97E-09
TraesCS3B02G376800	EXPA2	-3.43	1.03E-08
TraesCS3B02G120700	FLA11	-4.06	1.13E-08
TraesCS2A02G082500	IRX9	-4.36	1.35E-08
TraesCS6D02G158600	CSLA1	-3.57	5.19E-08
TraesCS2D02G091400	Unknown	-4.14	7.54E-08
TraesCS5D02G137300	GT3	-3.10	1.77E-07
TraesCS3D02G105500	FLA11	-3.80	2.79E-07
TraesCS2D02G080400	IRX9	-4.33	3.13E-07
TraesCS2A02G153000	PAE	-2.86	3.45E-07
TraesCS5A02G143800	GAUT7	-3.65	4.99E-07
TraesCS1D02G404700	FLA6	-3.28	1.03E-06
TraesCS6A02G131900	IRX15-like	-5.26	1.27E-06
TraesCS2D02G099900	PME	-8.49	1.48E-06
TraesCS4A02G227100	GXM-like	-7.37	1.62E-06
TraesCS5D02G107900	COBL-5B	-3.33	2.20E-06
TraesCS5D02G280400	CTL1	-2.22	2.68E-06
TraesCS6D02G121700	IRX15-like	-4.45	3.22E-06
TraesCS5A02G129800	GT3	-2.80	5.03E-06
TraesCS1D02G111600	FLA11	-7.80	7.85E-06
TraesCS4D02G086700	GXM1-like	-4.24	8.06E-06
TraesCS1B02G167200	CESA7-like	-3.04	9.85E-06



876

877 **Figure 7. Colonisation by *G. hyphopodioides* results in local downregulation of cell-**
 878 **wall related genes.** A. The top 30 most differentially expressed genes relating to cell wall
 879 organisation and biogenesis in *G. hyphopodioides* colonised plants at 5 dpi. Ordered by
 880 significance (padj); B. Gene counts of selected genes across time points; C. qPCR expression
 881 analysis of CESA7-like, COBL-5D and FLA11 in *G. hyphopodioides* colonised or *G. tritici*
 882 infected plants at 5 dpi (Log2FC relative to the mock inoculated control).

883